*Material Design & Processing Communications*

WILEY

RESEARCH ARTICLE OPEN ACCESS

# Influence of Fiber Content and Fiber Length on the Thermal and Electrical Properties of Kenaf Short Fiber–Reinforced Bulk Molding Compounds (BMCs) for Compression Molding

Subramaniasarma Sreenivasan | Mohd Khairol Anuar Mohd Ariffin | B. T. Hang Tuah Baharudin | Shamsuddin Sulaiman

Mechanical and Manufacturing Engineering Department, Faculty of Engineering, University Putra Malaysia, Serdang, Selangor D. E., Malaysia

**Correspondence:** Subramaniasarma Sreenivasan (s_sarma82@yahoo.com)

**Received:** 3 March 2026 | **Revised:** 23 April 2026 | **Accepted:** 29 May 2026

**Academic Editor:** Prashanth Konda Gokuldoss

**Keywords:** bulk molding compounds | heat deflection temperature | kenaf | thermal conductivity

## ABSTRACT

The recent trends have seen natural fiber–reinforced composites (NFRCs) garnering a large following due to their low density, commercial viability, low health risk, high tensile strength and modulus, and renewability. This paper discusses the thermal properties such as the thermal conductivity, heat deflection temperature, thermal stability, and dielectric strength of kenaf-reinforced bulk molding compound (BMC). The Lewis–Nielsen method was used to calculate theoretical values and compare with the experimental values. It has been found that the average thermal conductivity decreases as the fiber loading increases for all fiber lengths. The highest was observed in the BMC reinforced with 9-mm kenaf short fiber, with a value of 0.42. It has also been found that the heat deflection temperature decreases proportionally to the loading of the fiber due to varied fiber stress loading in the material. It was also found that fiber length did not play a significant part in the heat deflection temperature. From the DSC and TGA results, it can be said that thermal stability is preserved for all materials and peaks at 12 mm 20%. However, dielectric strength was found to be directly proportional to fiber loading as well as fiber length. The highest was at 15 mm 30% loading. It can be concluded that both fiber loading and fiber length play a significant part in the thermal and electrical properties of the composites.

## Highlights

- Thermal conductivity drops as fiber loading increases.
- Twelve-millimeter fibers give the best heat deflection performance at low loadings.
- Higher fiber loads reduce cure efficiency and increase cure variability.
- Dielectric strength improves slightly with longer fibers and higher loading.
- Optimal balance is found at moderate fiber content with midlength fibers.

## 1 | Introduction

Natural fiber–reinforced plastics (NFRPs) have attracted growing attention in recent decades due to their sustainability, low density, and competitive mechanical properties compared with synthetic fiber composites [1, 2]. Their adoption in industries such as automotive and aerospace has been driven

**TABLE 1** | Some NFRC car components.

| Vehicle part | Material used |
|---|---|
| Glove box | Wood/cotton fibers and molded, flax/sisal |
| Door panels | Flax/sisal with thermoset resin |
| Seat coverings | Leather/wool backing |
| Seat surface | Coconut fibers/natural rubber |
| Trunk panel | Cotton fibers |
| Trunk floor | Cotton fibers with PP/PET |
| Insulation | Cotton fibers |
| Floor panels | Flax mat with polypropylene |

**FIGURE 1** | 2018 Mercedes A class automotive NRFP components [5].

by the need to reduce environmental impact and improve recyclability [3–5]. For example, German automotive manufacturers account for nearly two-thirds of natural fiber use in Europe [6] with applications ranging from glove boxes and door panels to trunk liners and insulation materials (Table 1) as illustrated in Figure 1.

Among natural fibers, kenaf (*Hibiscus cannabinus*) has emerged as a particularly promising reinforcement material. Kenaf fibers combine high tensile strength, renewability, and cost-effectiveness, making them suitable for lightweight, eco-friendly composites [7, 8]. Studies have demonstrated that kenaf-reinforced composites can reduce vehicle weight, thereby improving fuel efficiency and lowering carbon emissions [7–10]. Advances in fiber surface treatments and hybridization with other fibers have further expanded their application scope in both structural and semistructural components [11, 12]. Recent work has also highlighted improvements in mechanical and thermal properties when kenaf is combined with polypropylene or epoxy matrices [13–15].

Despite these advantages, most prior work has focused on mechanical properties such as tensile strength, flexural modulus, and impact resistance [16–21]. In contrast, systematic investigations of thermal and electrical properties remain limited, even though these characteristics are critical for applications involving heat resistance, dimensional stability, and electrical insulation. For example, thermal conductivity and heat deflection temperature (HDT) determine suitability for automotive interior panels, whereas dielectric strength governs performance in electrical housings. Recent studies on silane-treated kenaf composites have shown that fiber length and loading significantly affect performance, but comprehensive benchmarking remains scarce [22].

Theoretical modeling provides an important complement to experimental work. The Lewis–Nielsen model has been widely applied to predict composite properties, accounting for filler geometry, packing density, and conductivity contrast [12], [23–25]. Extensions of this model have been successfully applied to polymer nanocomposites and hybrid systems, demonstrating its versatility for natural fiber composites [26, 27].

Although many studies have examined the thermal and electrical properties of natural fiber–reinforced polymer composites, the novelty of this research lies in its systematic investigation of both fiber length and fiber content in silane-treated kenaf bulk molding compounds (BMCs). By integrating experimental measurements of thermal conductivity, HDT, thermal stability, and dielectric strength with theoretical predictions from the Lewis–Nielsen model, this study provides a comprehensive framework that goes beyond single-property analyses commonly reported in the literature. This dual focus on fiber geometry and loading, combined with benchmarking against established models and prior studies, offers new insights into optimizing kenaf-based composites for multifunctional performance in industrial applications. By integrating experimental and theoretical approaches, this work provides new insights into optimizing kenaf BMCs for industrial applications, thereby advancing the broader adoption of natural fiber composites in sustainable engineering.

## 2 | Materials and Methodology

### 2.1 | Materials

The BMC was prepared using a twin Z-blade mixer at Wah Ma Chemical Sdn. Bhd., Penang, Malaysia. Kenaf fibers were prepared at Universiti Putra Malaysia using a custom-built fiber cutting machine. The fibers were chopped to the specified lengths and surface treated with 0.6 wt.% 3-glycidyloxypropyltrimethoxysilane (GPTMS) for 24 h at room temperature (24°C). Following treatment, the fibers were oven-dried at 85°C for 24 h to remove residual moisture prior to compounding.

The resin used was isophthalic unsaturated polyester (UP). Isophthalic UP resin offers several advantages when employed in bulk BMCs. Compared with orthophthalic resins, isophthalic UP resins exhibit superior chemical resistance, enhanced mechanical strength, and improved thermal stability, making them particularly suitable for demanding applications. Their higher resistance to hydrolysis and solvents ensures long-term durability, whereas the resin's ability to achieve excellent fiber wet-out contributes to uniform dispersion and strong interfacial bonding with natural fibers such as kenaf. In addition, isophthalic UP resins provide better dimensional stability under heat and load, which is critical for maintaining performance in compression-molded parts. These attributes make isophthalic UP resin an ideal matrix for developing eco-friendly, high-performance

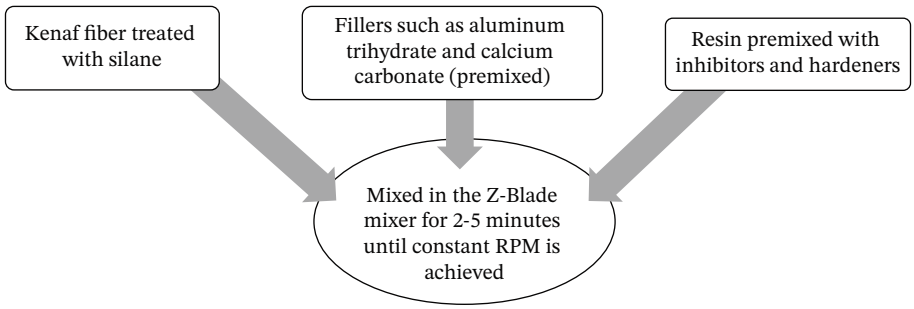


**FIGURE 2** | Preparation of kenaf-reinforced BMC.

**FIGURE 3** | Mixing kenaf-reinforced BMC.

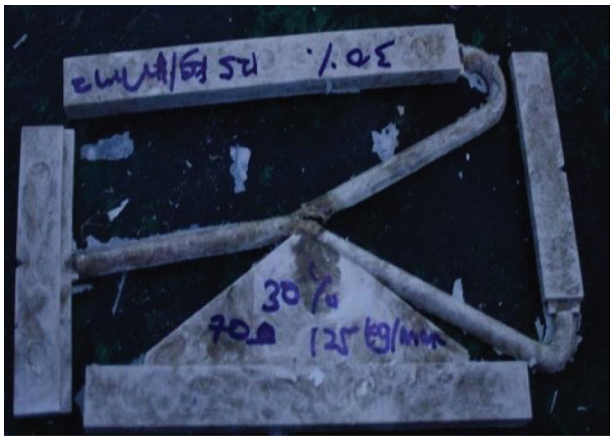

**FIGURE 4** | Molded samples.

composites that balance sustainability with industrial reliability. The UP resin, inhibitors, hardeners, and the fillers were obtained from Wah Ma Chemicals Sdn. Bhd., Penang Malaysia. All three materials were then mixed using a twin Z-blade mixture for about 2–5 min until constant RPM of the mixing blades is achieved. The mixing methodology is further elaborated in Figure 2. Figure 3 shows the BMC preparation in the twin Z-blade mixing machine.

The fiber–matrix interfacial interactions in the kenaf–polyester system have been previously investigated by the authors using direct micromechanical and morphological techniques. In our earlier work, interfacial shear strength (IFSS) was quantitatively evaluated using microdroplet pull-out tests, whereas scanning electron microscopy (SEM) was employed to assess fiber surface morphology and fiber–matrix adhesion. Alkali treatment was shown to remove surface impurities and lignin, increasing surface roughness and effective aspect ratio, thereby enhancing mechanical interlocking. Silane treatment further improved interfacial bonding through chemical coupling between fiber hydroxyl groups and the UP matrix, resulting in increased IFSS. SEM observations confirmed improved wettability and reduced interfacial voids for treated fibers. These interfacial mechanisms are directly applicable to the kenaf short fiber BMC system studied herein and provide a mechanistic basis for the observed dependence of thermal and electrical properties on fiber content and fiber length [28–30].

The mixture was then stored for 24 h at 20°C for stabilization. After stabilization, the BMC was used to mold the separate pieces required for the experimental tests. They were molded using an 85-ton vertical injection–compression molding machine at 185°C. Figure 4 shows the molded pieces.

In this study, fiber lengths of 9, 12, and 15 mm were selected to balance reinforcement efficiency with ease of processing. Shorter fibers (9 mm) mix readily with the resin and disperse uniformly, whereas medium fibers (12 mm) are close to the critical length reported in natural fiber composites for effective stress transfer between fiber and matrix [28, 31, 32]. Longer fibers (15 mm) were included to explore whether extended reinforcement could further enhance thermal and electrical properties. However, preliminary trials showed that fibers longer than 15 mm created significant challenges during mixing, including poor resin wet-out and high fiber breakage, which compromised composite uniformity. By limiting the study to this range, we ensured that the materials tested were both scientifically meaningful and practically feasible, consistent with prior findings on critical fiber length in kenaf composites [33].

## 2.2 | Methods

### 2.2.1 | Theoretical Calculations

The Lewis–Nielsen method is a well-established analytical approach for predicting the mechanical and thermal properties of composite materials. It is commonly used to estimate properties such as elastic modulus and thermal conductivity for composites reinforced with particulate or fibrous fillers. Unlike simpler predictive models, such as the rule of mixtures, the Lewis–Nielsen

**TABLE 2** | Theoretical thermal conductivity constants.

| $K_f$ | $K_m$ | $\phi_{max}$ | $A$ | $B$ | $V_f$(10%) | $V_f$(20%) | $V_f$(30%) |
|---|---|---|---|---|---|---|---|
| 0.2 | 0.5 | 0.52 | 2 | 0.66667 | 0.1901 | 0.3455 | 0.4750 |

model incorporates the effects of filler shape, size, and volume fraction, enabling more accurate property estimation. Importantly, the model accounts for interactions between the matrix and the filler, providing reliable predictions for both mechanical and thermal behavior [12].

The applicability of the Lewis–Nielsen method extends to a wide range of composite systems, including polymer-based composites, ceramic composites, and natural fiber–reinforced materials [23, 24]. A key advantage of the model is its consideration of filler geometry (e.g., spherical, cylindrical, or platelet shaped), which allows more precise predictions, particularly for anisotropic fillers [25, 34]. In addition, the model is relatively simple to implement and does not require complex numerical computation, making it practical for both academic research and industrial applications. Table 2 shows the constants that were used in the theoretical calculations. The equations used are listed below:

$$\frac{k_{\text{eff}}}{k_m} = \frac{1 + ABV_f}{1 - B\psi V_f} \tag{1}$$

$$B = \frac{k_f/k_m - 1}{(k_f/k_m) + A} \tag{2}$$

$$\psi = 1 + \left( \frac{1 - \phi_{\text{maxx}}}{\phi^2_{\text{maxx}}} \right) V_f \tag{3}$$

where

$k$ = thermal conductivity.

eff = effective (composite).

$m$ = matrix.

$f$ = fiber.

$V$ = volumetric fraction.

$A$ = shape factor, randomly oriented fibers.

$B$ = a parameter related to the contrast in thermal conductivity between the fiber and matrix.

$\psi$ = a parameter that accounts for the maximum packing fraction of the fibers.

### 2.2.2 | Experimental Methods

The thermal conductivity tests were performed at TNB Research Sdn. Bhd. using a Hukseflux THASYS Thin Heater Apparatus for thermal conductivity measurement under ASTM C1114. The thin plastic pieces were premolded at Wah Ma Chemicals Sdn. Bhd. The samples were 6 × 6 cm with a thickness of 2 mm. Figure 5 shows the thermal conductivity sample. The heat deflection tests were conducted using a Gotech HVA200A Computer HDT/VICAT Tester according to ASTM D648 using bar-shaped specimens. The dimensions of the test bars (127 × 13 × 3 mm) and the test procedure conformed to the ASTM D648-06 standard. The loading pressure was 1.82 MPa, and samples were heated at a rate of 2°C/min from room temperature.

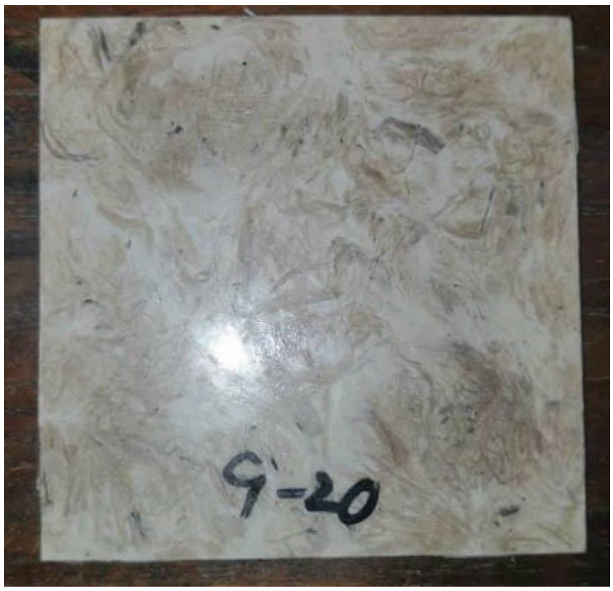


**FIGURE 5** | Thermal conductivity sample.

The calorimetric analysis was conducted using the TA Instruments DSC Q20 Differential Scanning Calorimeter (DSC) model used for calorimetric applications. The material sample was loaded onto the Tzero Measuring pan. The temperature was increased from 20°C to 200°C at 10°C per minute in accordance with ASTM D3418. The tests were then repeated three to five times to ensure the repeatability of the tests. Thermogravimetric analysis (TGA) was carried out using TA Instruments TGA Q500 analyzer to determine the thermal stabilities of the BMC by measuring the degradations of the compound through the mass loss coupled with temperature increase. The entirety of the specimens used were between 14 and 30 mg. The experiments were conducted while heating the samples from 30°C to 1000°C at the rate of 10°C/min in nitrogen. DSC and TGA were conducted at the Institute of Tropical Forestry and Forest Products, UPM. The dielectric strength test was also conducted using a 700-D149 Series-Dielectric Breakdown Tester according to ASTM D149 using plate-shaped specimens. The 2-mm-thickness specimens were loaded into the machine, and the voltage was increased at a rate of 100 V/s until dielectric breakage occurred. The resin which was provided by Wah Ma Chemicals Sdn. Bhd had a heat copolymerization of 275 J/g. For each of the

tests above, a minimum of five repetitions were done, and the averages were obtained.

## 3 | Results and Discussions

### 3.1 | Thermal Conductivity

Figure 6 shows the variation in thermal conductivity as a function of kenaf fiber content for all three fiber lengths investigated. The UP matrix exhibits a baseline thermal conductivity of approximately 0.50 W/m·K. The incorporation of kenaf fibers results in a consistent reduction in thermal conductivity, with composites containing 10 wt.% fiber achieving values of approximately 0.42 W/m·K for the 9-mm fiber length. With increasing fiber content, conductivity further decreases, reaching values in the range of 0.11–0.16 W/m·K at 30 wt.% loading. This reduction is primarily attributed to the hollow cellular microstructure of kenaf fibers, which introduces low-conductivity pathways, as well as the presence of hydroxyl groups that impede heat transfer relative to the neat resin [20]. These observations are in good agreement with the work of Paul et al., who reported similar decreases in thermal conductivity with increasing natural fiber incorporation [31].

The predictions obtained using the Lewis–Nielsen model show good agreement with the experimental thermal conductivity data, confirming its suitability for natural fiber–reinforced composite system [24, 35]. Table 3 presents a comparison of thermal conductivity ranges reported for various natural fiber composites. This benchmarking highlights the competitive performance of kenaf-based composites, with reported values for jute ranging from 0.18 to 0.14 W/m·K [19], bamboo from 0.21 to 0.19 W/m·K [20], and luffa from 0.20 to 0.10 W/m·K [17]. In comparison, kenaf composites exhibit a wider conductivity range (0.42–0.11 W/m·K), indicating that processing conditions, fiber dispersion, and fiber–matrix interfacial quality play a significant role in governing thermal behavior. By contrast, E-glass fiber composites exhibit substantially higher thermal conductivity (≈0.9 W/m·K) [31, 36], underscoring the advantage of kenaf fibers for thermal insulation applications.

### 3.2 | HDT

Table 4 summarizes the HDT and dielectric strength measured at 1.82 MPa for GPTMS-treated kenaf-reinforced UP composites. The results show that HDT is dependent on both fiber content and fiber length, with distinct trends observed at each loading level.

At 10 wt.% fiber content, HDT increases with fiber length, rising from 95.68°C at 9 mm to a maximum of 100.30°C at 12 mm, before decreasing slightly to 96.58°C at 15 mm. This trend indicates that a fiber length of approximately 12 mm is close to the critical fiber length required for efficient stress transfer in the GPTMS-treated system. At this length, improved fiber–matrix interfacial bonding more effectively restricts polymer chain mobility, thereby enhancing resistance to thermally induced deformation. The low experimental error (1.25%–1.91%) confirms good measurement repeatability and the reliability of the observed trend.

When the fiber content is increased to 20 wt.%, HDT values decrease and fall within a narrower range of 92.28°C–94.36°C, with only a weak dependence on fiber length. This reduction suggests that although GPTMS treatment improves interfacial adhesion, the higher fiber fraction reduces matrix continuity and increases fiber–fiber interactions. These effects limit the

**TABLE 3** | Thermal conductivity comparisons.

| Fiber | Loading, % | Thermal conductivity, W/m·K | Source |
|---|---|---|---|
| Luffa | 10%–25% | 0.20–0.10 | [17] |
| Narrowleaf cattail | 15%–32% | 0.38–0.31 | [18] |
| Jute | 10%–40% | 0.18–0.14 | [19] |
| Bamboo | 15%–30% | 0.21–0.19 | [20] |
| Kenaf | 10%–30% | 0.42–0.11 | This study |
| E glass | 5%–15% | 0.93–0.88 | [21] |

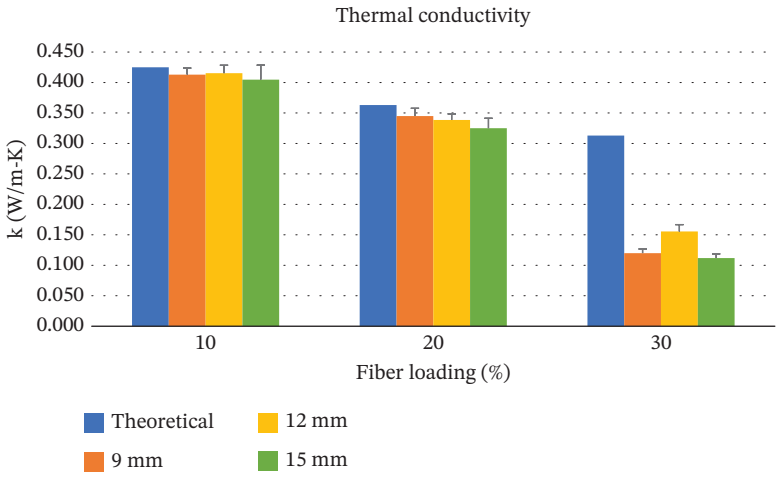


**FIGURE 6** | Thermal conductivity graph.

**TABLE 4** | Heat deflection temperature and dielectric strength results.

| Fiber by weight percentage | Fiber length (mm) | HDT (°C at 1.82 MPa) | | Dielectric strength (kV) | |
|---|---|---|---|---|---|
| | | Value | Error (%) | Value | Error (%) |
| 10% | 9 | 95.68 | 1.25% | 27 | 0.6% |
| | 12 | 100.30 | 1.79% | 28 | 0.8% |
| | 15 | 96.58 | 1.91% | 29 | 1.2% |
| 20% | 9 | 92.84 | 2.54% | 29 | 3.75% |
| | 12 | 92.28 | 1.35% | 29 | 2.36% |
| | 15 | 94.36 | 1.40% | 30 | 4.52% |
| 30% | 9 | 87.78 | 1.94% | 29 | 2.15% |
| | 12 | 85.46 | 1.14% | 29 | 2.63% |
| | 15 | 81.26 | 2.13% | 30 | 2.33% |

composite's ability to uniformly distribute thermal and mechanical stresses, resulting in lower HDT compared with the 10 wt.% formulations.

At 30 wt.% fiber content, the decline in HDT becomes more pronounced, with values decreasing monotonically from 87.78°C at 9 mm to 81.26°C at 15 mm. At this high fiber loading, the composite behavior becomes increasingly fiber dominated, and longer fibers exacerbate dispersion difficulties, fiber entanglement, and local stress concentrations. Such conditions reduce interfacial load-transfer efficiency and accelerate deformation during thermal softening. This behavior is consistent with micromechanical interpretations based on shear-lag theory, where excessive fiber content leads to ineffective stress transfer due to insufficient surrounding matrix and increased likelihood of fiber agglomeration. Similar trends have been reported in other silane-treated natural fiber composites, where high fiber loading promotes microstructural nonuniformity and reduced thermo-mechanical performance [28, 32].

The variation in HDT with fiber length differs between low–moderate (10%–20%) and high (30%) fiber loadings due to changes in matrix continuity and interfacial efficiency. At 10% and 20% loading, increasing fiber length up to 12 mm improves stress transfer and restricts polymer chain mobility, resulting in increased HDT. Beyond this length, fiber dispersion becomes less uniform, reducing effective interfacial reinforcement. At 30% fiber loading, matrix continuity is significantly reduced and fiber–fiber interactions dominate. Increasing fiber length under these conditions leads to poorer dispersion, increased stress concentrations, and reduced interfacial efficiency, causing a monotonic decrease in HDT.

Despite these reductions, the overall trends confirm that GPTMS treatment remains beneficial. At low to moderate fiber contents, enhanced interfacial bonding helps maintain HDT values above those typically reported for untreated or weakly bonded systems. These observations are consistent with earlier studies on surface-treated natural fiber composites, which similarly report optimal thermo-mechanical performance at moderate fiber loadings and near-critical fiber lengths [22, 37]. Moreover, the small experimental error margins, all below 2.6%, demonstrate good measurement, repeatability, and stability of the HDT results.

### 3.3 | Dielectric Strength

Surface modification of kenaf fibers using GPTMS plays a critical role in governing the dielectric behavior of kenaf-reinforced BMC composites. During hydrolysis and condensation reactions, the silane coupling agent forms siloxane bonds with hydroxyl groups on the cellulose surface, thereby reducing fiber hydrophilicity and enhancing fiber–matrix interfacial adhesion [38, 39]. Improved interfacial integrity minimizes the formation of microvoids and interfacial defects, which otherwise act as charge-trapping sites and local electric-field intensification regions that can accelerate dielectric breakdown. The beneficial influence of silane treatment on dielectric properties has been widely reported in natural fiber composites, with treated fibers consistently exhibiting improved dielectric performance and enhanced electrical stability under applied electric fields [40].

The dielectric strength values presented in Table 4 indicate that both fiber content and fiber length influence electrical breakdown behavior. The dielectric strength values listed in Table 4 indicate that fiber length has only a modest influence on electrical breakdown behavior. Across all fiber loadings, dielectric strength remains within a narrow range of 27–30 kV/mm, with a slight increase observed as fiber length increases from 9 to 15 mm. However, the magnitude of this variation is small and remains within experimental error, indicating that dielectric performance is relatively insensitive to fiber length compared with thermal-mechanical properties such as HDT.

The weak dependence on fiber length suggests that GPTMS treatment effectively stabilizes the fiber–matrix interface, minimizing electrically active defects such as voids and interfacial

discontinuities even at longer fiber lengths. In contrast to HDT, which is strongly governed by stress-transfer efficiency and matrix continuity, dielectric strength is primarily controlled by overall insulation continuity and interfacial integrity, both of which remain largely preserved across the fiber length range investigated. Dielectric behavior is also influenced by the chemistry of the wet polyester matrix, comprising UP resin, styrene monomer, a para-benzoquinone inhibitor, and dual peroxide initiators (tert-butyl peroxybenzoate and tert-butyl peroxy-2-ethylhexanoate). Together, these components support uniform free-radical crosslinking and the formation of a stable, homogeneous polymer network, which is essential for maintaining dielectric strength under high electric-field conditions [41]. The inclusion of aluminum hydroxide and calcium carbonate fillers further enhances insulating performance by increasing the tortuosity of electrical conduction pathways, restricting charge mobility, and improving thermal stability during electrical breakdown. Similar filler-induced improvements have been reported in polyester-based and other polymer insulation systems [42, 43].

Overall, these findings demonstrate that well-engineered, GPTMS-treated kenaf/polyester BMCs can achieve dielectric strength levels comparable to those reported for other natural fiber-based insulating composites, supporting their potential application in semistructural electrical insulation components [44].

## 3.4 | Thermal Behavior and Cure Characteristics of Silane-Treated Kenaf/UP BMC

Differential scanning calorimetry (DSC) and TGA were used to investigate the influence of fiber loading and fiber length on the thermal behavior and curing characteristics of silane-treated kenaf fiber–reinforced UP BMC. A typical DSC thermogram shows three distinct thermal features: the glass transition temperature ($T_g$), the exothermic curing reaction peak temperature ($T_{CR}$), and the residual heat of reaction ($\Delta H_r$). These parameters provide insight into the evolution of polymer network structure and the degree of cure in the presence of lignocellulosic fibers. Figure 7 shows the DSC curve for the kenaf-reinforced BMC with 12-mm fiber and 10% loading.

### 3.4.1 | DSC: Effect of Fiber Loading on Curing Behavior

The DSC results show that increasing kenaf fiber content leads to a gradual increase in the $T_g$ of the composites. The $T_g$ rises from approximately 102°C at 10 wt.% fiber loading to about 105°C–110°C at 30 wt.%, indicating that the incorporation of fibers restricts polymer chain mobility and increases the apparent rigidity of the polymer network. This behavior is commonly observed in natural fiber–reinforced thermoset systems and is typically attributed to physical confinement of the polymer chains, as well as enhanced interfacial interactions between the fiber and matrix [2, 37].

In contrast, the degree of cure exhibits an opposite trend. The cure percentage decreases from approximately 78%–83% at 10–20 wt.% fiber loading to values as low as 66% at 30 wt.%. This inverse relationship indicates that higher fiber contents hinder the curing process. Lignocellulosic fibers contain hydroxyl groups, residual moisture, and extractives such as lignin and hemicellulose, which can interfere with free-radical polymerization by acting as radical scavengers or by restricting resin mobility [45, 46]. Consequently, the curing reaction becomes less efficient and increasingly heterogeneous as fiber content increases.

The $\Delta H_r$ further supports this interpretation. While $\Delta H_r$ values remain relatively consistent at low fiber loadings, they exhibit significant dispersion at 30 wt.% fiber loading, reflecting nonuniform curing behavior. This suggests the coexistence

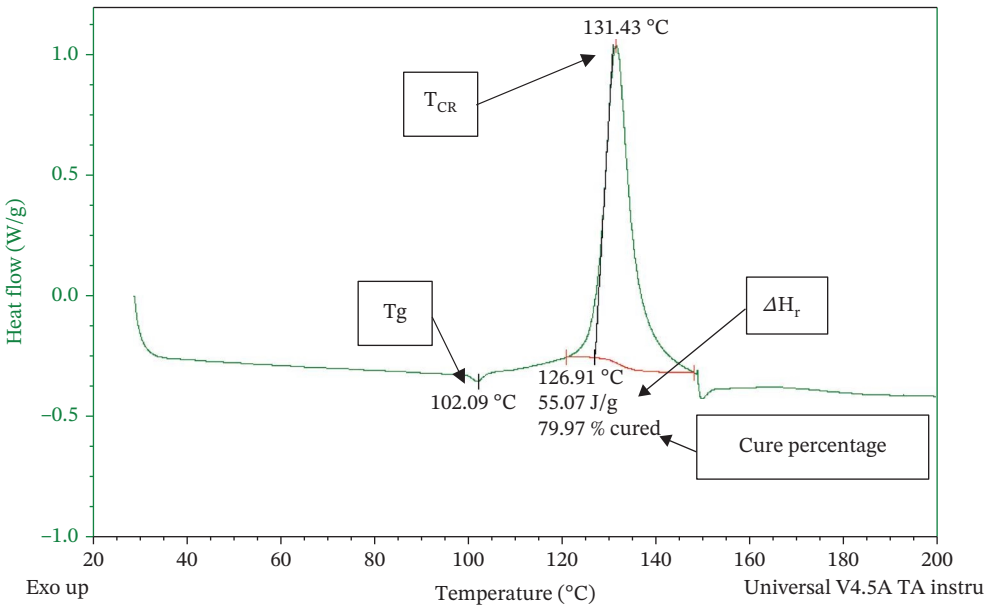


**FIGURE 7** | Typical DSC thermogram of the kenaf–polyester BMC.

**TABLE 5** | Differential scanning calorimetry analysis results.

| Fiber by weight percentage | Fiber length (mm) | Code | DSC analysis results | | | |
|---|---|---|---|---|---|---|
| | | | $\Delta H_r$(J/g) | $T_g$(°C) | $T_{CR}$(°C) | Cure % |
| 10% | 9 | K9-1 | 51.99 | 98.43 | 131.20 | 81.09 |
| | 12 | K12-1 | 55.07 | 102.09 | 131.43 | 79.97 |
| | 15 | K15-1 | 59.13 | 107.01 | 139.56 | 78.50 |
| 20% | 9 | K9-2 | 45.22 | 102.57 | 130.27 | 83.56 |
| | 12 | K12-2 | 53.08 | 105.57 | 134.91 | 80.70 |
| | 15 | K15-2 | 61.55 | 109.09 | 139.00 | 77.62 |
| 30% | 9 | K9-3 | 46.38 | 101.29 | 132.82 | 83.14 |
| | 12 | K12-3 | 76.71 | 104.01 | 133.01 | 72.10 |
| | 15 | K15-3 | 93.49 | 110.65 | 138.62 | 66.00 |

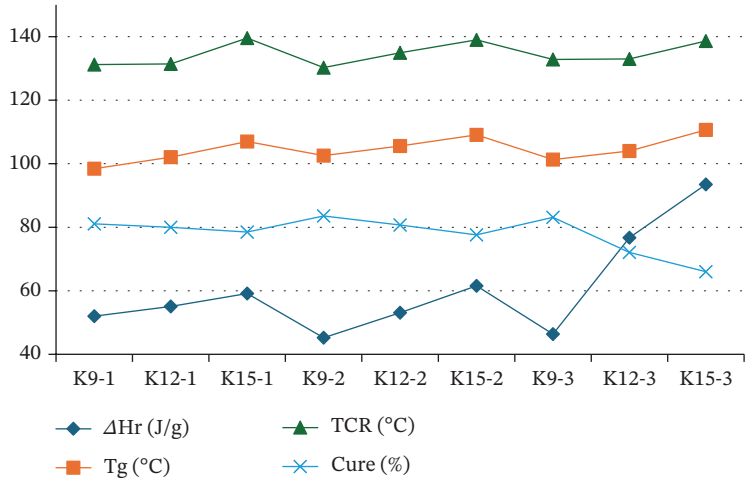


**FIGURE 8** | DSC analysis comparison of the different kenaf–polyester BMC.

of resin-rich and fiber-rich regions within the composite, a phenomenon frequently reported in highly filled natural fiber composites [47]. Such microstructural heterogeneity indicates that increasing fiber content not only enhances reinforcement but also alters the curing environment and network development.

In addition, $T_{CR}$ shows a slight upward shift with increasing fiber content, indicating that higher thermal energy is required to sustain the curing reaction in fiber-rich systems. This shift can be attributed to the low thermal conductivity of kenaf fibers and the physical barrier they introduce to heat transfer and radical diffusion. Similar increases in cure temperature have been reported for natural fiber–reinforced thermoset composites, where fiber incorporation modifies the kinetics of crosslinking reactions [48]. A comprehensive comparison of these thermal parameters is presented in Table 5, with Figure 8 providing a graphical representation that highlights the observed trends across different fiber loadings and fiber.

### 3.4.2 | TGA: Thermal Stability and Degradation Behavior

TGA provides additional insight into the thermal stability of the kenaf/UP BMC system. The onset degradation temperature ($T_{on}$) shows a slight decrease with increasing fiber content, shifting from approximately 228°C at 10 wt.% fiber loading to around 217°C at 30 wt.%. This trend is attributed to the inherently lower thermal stability of lignocellulosic fibers compared with the polyester matrix, as hemicellulose and cellulose typically undergo thermal degradation at lower temperatures than thermoset polymers [2, 46].

Despite the reduction in $T_{on}$, the maximum degradation temperature ($T_{max}$) remains relatively stable across all compositions, varying only between approximately 357°C and 363°C. This stability indicates that the primary degradation mechanism of the polyester matrix is largely preserved following fiber incorporation. The relatively constant $T_{max}$ suggests that while the presence of kenaf fibers influences the onset of thermal degradation,

**TABLE 6** | Thermogravimetric analysis results.

| Length/Type | Neat kenaf | 9 mm | | | 12 mm | | | 15 mm | | |
|---|---|---|---|---|---|---|---|---|---|---|
| **Loading** | **100%** | **10%** | **20%** | **30%** | **10%** | **20%** | **30%** | **10%** | **20%** | **30%** |
| $T_{on}$ (°C) | 150 | 228.58 | 223.08 | 218.32 | 232.64 | 222.38 | 220.68 | 223.96 | 219.88 | 217.82 |
| $T_{\max}$ (°C) | 350 | 361.25 | 360.66 | 357.14 | 363.30 | 358.45 | 357.42 | 361.46 | 360.47 | 358.19 |
| $W_0$ (%) | 100% | 28.13 | 35.20 | 40.95 | 27.87 | 34.16 | 41.44 | 28.76 | 32.13 | 40.49 |
| $W_f$ (%) | NA | 45.20 | 39.05 | 32.84 | 44.94 | 38.44 | 33.29 | 45.59 | 38.94 | 34.15 |

it does not fundamentally alter the dominant thermal decomposition pathway of the matrix.

The residual mass ($W_f$) increases noticeably with fiber loading, reflecting the enhanced char formation associated with lignocellulosic fibers. Natural fibers are known to promote char development during thermal degradation due to their high carbon content, resulting in increased $W_f$ at elevated temperatures [37]. In addition, the presence of silane-treated fiber–matrix interfaces may further contribute to improved thermal residue through stronger interfacial bonding and reduced volatilization during degradation.

Fiber length also has a measurable influence on the thermal behavior of the composites. Systems reinforced with 12-mm fibers exhibit slightly higher $T_{on}$ and $T_{\max}$ values compared with those containing 9 and 15-mm fibers. This suggests that an intermediate fiber length promotes more uniform fiber dispersion and more effective interfacial bonding, leading to improved thermal stability. Similar behavior has been reported in fiber-reinforced composite systems, where optimal fiber length enhances microstructural uniformity and load transfer efficiency, thereby improving resistance to thermal degradation [38]. The detailed thermogravimetric parameters, including $T_{on}$, $T_{\max}$, and $W_f$, are summarized in Table 6, which supports the observed trends in thermal stability with varying fiber content and fiber.

### 3.4.3 | Role of Silane Treatment and Microstructural Implications

The kenaf fibers used in this study were surface modified with GPTMS, which plays a key role in tailoring the fiber–matrix interface. Silane coupling agents are well known for enhancing interfacial adhesion through the formation of covalent bonds between hydroxyl groups on the fiber surface and the surrounding polymer matrix [28, 38]. In the present system, GPTMS treatment likely contributes to the observed increase in $T_g$ and the improved thermal stability at moderate fiber loadings by strengthening fiber–matrix interactions and restricting polymer chain mobility near the interface.

However, the persistence of cure heterogeneity at high fiber loadings indicates that silane treatment alone is insufficient to fully mitigate the inherent limitations associated with lignocellulosic fibers, such as residual moisture, surface polarity, and chemical heterogeneity. At elevated fiber contents, resin impregnation becomes increasingly constrained, promoting fiber agglomeration and the formation of resin-starved regions. These microstructural features are expected to manifest in SEM observations as interfacial gaps, fiber pull-out, and voids—characteristics that have been widely reported in natural fiber–reinforced composites at high fiber loadings [47].

### 3.4.4 | Implications for BMC Processing

From a processing standpoint, the combined DSC and TGA results emphasize the critical role of fiber content and fiber length in governing the manufacturability of kenaf-reinforced BMCs. The observed increase in $T_{CR}$ alongside the reduction in degree of cure at higher fiber loadings indicates that conventional curing cycles may be inadequate for highly filled systems. Under these conditions, extended curing times or increased mold temperatures may be necessary to achieve uniform crosslinking throughout the composite.

At the same time, the reduction in $T_{on}$ with increasing fiber content highlights the need for careful control of processing conditions to avoid premature thermal degradation of the lignocellulosic fibers. These results therefore point to the existence of a defined processing window in which fiber content and fiber length must be judiciously balanced to ensure adequate curing, thermal stability, and processability.

Taken together, the DSC and TGA indicate that moderate fiber loading combined with an intermediate fiber length provides the most favorable balance of curing behavior and thermal resistance in GPTMS-treated kenaf/UP BMC systems. Although higher fiber contents offer increased reinforcement potential, excessive loading leads to cure heterogeneity and reduced thermal stability at the onset of degradation. These findings underscore the importance of optimizing fiber content, fiber geometry, and interfacial chemistry during the design and processing of natural fiber–reinforced BMCs.

## 4 | Conclusions

This study systematically evaluated the influence of kenaf fiber content and fiber length on the thermal and electrical properties of kenaf short fiber–reinforced BMC. The experimental results clearly demonstrate that both parameters play a critical role in governing the structure–property relationships of the composite system.

Thermal characterization revealed that increasing fiber content contributes to enhanced thermal rigidity and resistance

to deformation, as reflected by the observed trends in thermal stability. This behavior is primarily associated with the ability of kenaf fibers to restrict polymer chain mobility within the matrix. However, at higher fiber loadings, issues such as fiber agglomeration and reduced matrix wetting become more pronounced, which may limit further improvements in thermal performance and adversely affect processability.

Fiber length was also found to significantly influence the thermal response of the composites. Longer fibers promote improved interfacial bonding and load transfer, resulting in a more continuous reinforcement network that modifies thermal transport pathways within the BMC. In contrast, shorter fibers, while offering better dispersion, provide reduced reinforcement continuity and therefore contribute less effectively to thermal performance enhancement.

Electrical characterization showed that the incorporation of kenaf fibers alters the insulating behavior of the BMC composites. The addition of natural fibers increases the overall electrical resistivity of the material, which can be attributed to the inherently insulating nature of kenaf fibers and the disruption of potential conductive pathways within the polymer matrix. Both fiber content and fiber length influence electrical performance, with higher fiber loadings and optimized fiber lengths contributing to improved insulation characteristics.

Overall, the findings confirm that kenaf short fiber–reinforced BMCs exhibit tunable thermal and electrical properties through careful control of fiber content and fiber length. These results highlight the potential of kenaf-based BMCs as sustainable alternatives to conventional composite materials in applications requiring enhanced thermal stability and electrical insulation. Future work should focus on further optimizing fiber–matrix interfacial adhesion, evaluating long-term thermal aging behavior, and elucidating process–property relationships to advance material performance and industrial applicability.


### Funding

No funding was received for this manuscript.


### Conflicts of Interest

The authors declare no conflicts of interest.

### Data Availability Statement

The data that support the findings of this study are available from the corresponding author upon reasonable request.

### References


1. O. Akampumuza, P. M. Wambua, A. Ahmed, W. Li, and X. H. Qin, "Review of the Applications of Biocomposites in the Automotive Industry," *Polymer Composites* 38, no. 11 (2017): 2553–2569, https://doi.org/10.1002/pc.23847.

2. O. Faruk, A. K. Bledzki, H. P. Fink, and M. Sain, "Biocomposites Reinforced With Natural Fibers: 2000–2010," *Progress in Polymer Science* 37, no. 11 (2012): 1552–1596, https://doi.org/10.1016/j.progpolymsci.2012.04.003.

3. J. Holbery, and D. Houston, "Natural-Fiber-Reinforced Polymer Composites in Automotive applications," *JOM* 58, no. 11 (2006): 80–86, https://doi.org/10.1007/s11837-006-0234-2.

4. D. H. Mueller, and A. Krobjilowski, "Improving the Impact Strength of Natural Fiber Reinforced Composites by Specifically Designed Material and Process Parameters," *International Nonwoven Journal* 13, no. 4 (2004): 31–38, https://doi.org/10.1177/1558925004os-1300405.

5. V. Naik, M. Kumar, V. Vijayan, and A. Kaup, "A Review on Natural Fiber Composite Material in Automotive Applications," *Engineered Science* 18 (2022): 1–10, https://doi.org/10.30919/es8d655.

6. S. A. Ibraheem, A. Ali, and K. Abdan, "Development of Green Insulation Boards From Kenaf Fibres Part 2: Characterizations of Thermal and Water Absorption," *Key Engineering Materials* 462–463 (2011): 1331–1336, https://doi.org/10.4028/www.scientific.net/KEM.462-463.1331.

7. D. U. Shah, "Developing Plant Fibre Composites for Structural Applications by Optimising Composite Parameters: A Critical Review," *Journal of Materials Science* 48, no. 18 (2013): 6083–6107, https://doi.org/10.1007/s10853-013-7458-7.

8. M. P. M. Dicker, P. F. Duckworth, A. B. Baker, G. Francois, M. K. Hazzard, and P. M. Weaver, "Green Composites: A Review of Material Attributes and Complementary Applications," *Composites Part A: Applied Science and Manufacturing* 56 (2014): 280–289, https://doi.org/10.1016/j.compositesa.2013.10.014.

9. F. P. La Mantia, and M. Morreale, "Green Composites: A Brief Review," *Composites Part A: Applied Science and Manufacturing* 42, no. 6 (2011): 579–588, https://doi.org/10.1016/j.compositesa.2011.01.017.

10. L. Mohammed, M. N. M. Ansari, G. Pua, M. Jawaid, and M. S. Islam, "A Review on Natural Fiber Reinforced Polymer Composite and Its Applications," *International Journal of Polymer Science* 2015 (2015): 243947, https://doi.org/10.1155/2015/243947.

11. N. Saba, M. T. Paridah, K. Abdan, and N. A. Ibrahim, "Dynamic Mechanical Properties of Oil Palm Nano Filler/Kenaf/Epoxy Hybrid Nanocomposites," *Construction and Building Materials* 124 (2016): 133–138, https://doi.org/10.1016/j.conbuildmat.2016.07.059.

12. Y. Zhang, Y. Li, H. Ma, and T. Yu, "Tensile and Interfacial Properties of Unidirectional Flax/Glass Fiber Reinforced Hybrid Composites," *Composites Science and Technology* 88 (2013): 172–177, https://doi.org/10.1016/j.compscitech.2013.08.037.

13. C. H. Lee, S. M. Sapuan, and M. R. Hassan, "Mechanical and Thermal Properties of Kenaf Fiber Reinforced Polypropylene/Magnesium Hydroxide Composites," *Journal of Engineered Fibers and Fabrics* 12, no. 2 (2017): 155892501701200206, https://doi.org/10.1177/155892501701200206.

14. T. T. Silva, M. P. Ribeiro, L. D. Neuba, et al., "Tensile and Dynamic Toughness of Kenaf Fiber-Reinforced Epoxy Composites," *Fibers* 13, no. 9 (2025): 120, https://doi.org/10.3390/fib13090120.

15. G. Koronis, A. Silva, and M. Fontul, "Green Composites: A Review of Adequate Materials for Automotive Applications," *Composites Part B: Engineering* 44, no. 1 (2013): 120–127, https://doi.org/10.1016/j.compositesb.2012.07.004.

16. K. V. Rijswijk, W. D. Brouwer, and A. Beukers, *Application of Natural Fibre Composites in the Development of Rural Societies* (Delft University of Technology, 2001).

17. S. N. Hameed, and W. B. Salih, "Enhancing Mechanical and Thermal Properties of Unsaturated Polyester Resin With Luffa Fiber Reinforcements: A Volumetric Analysis," *Journal of Composite and Advanced Materials* 33, no. 6 (2023): 357–362, https://doi.org/10.18280/rcma.330602.

18. K. Ramanaiah, A. V. Ratna Prasad, and K. H. C. Reddy, "Mechanical Properties and Thermal Conductivity of Typha angustifolia Natural

Fiber–Reinforced Polyester Composites," *International Journal of Polymer Analysis and Characterization* 16, no. 7 (2011): 496–503, https://doi.org/10.1080/1023666X.2011.598528.

19. B. V. Subrahmanyam, S. V. Gopala Krishna, R. Jithedra Kumar, and S. B. R. Devireddy, "Experimental and Micromechanical ThermalCharacteristics of Jute Fiber Reinforced Polyester Composites," *Materials Today: Proceedings* 18 (2019): 350–356, https://doi.org/10.1016/j.matpr.2019.06.311.

20. M. Mounika, K. Ramanaiah, K. Mohana Rao, A. V. Ratna Prasad, and K. H. C. Reddy, "Thermal Conductivity Characterization of Bamboo Fiber Reinforced Polyester Composite," *Journal of Materials and Environmental Science* 3, no. 6 (2012): 1109–1116.

21. B. Bertoncelj, K. Vojisavljević, M. Vrabelj, and B. Malič, "Thermal Properties of Polymer-Matrix Composites Reinforced With E-Glass Fibers," *Informatica Biomedica/Journal of Microelectronics, Electronic Components and Materials* 45, no. 3 (2015): 216–221.

22. M. M. Mohd Ghaztar, N. N. I. Nik Ibrahim, and A. Z. Romli, "Sodium Hydroxide/Silane Treated Kenaf Fibre in Unsaturated Polyester Matrix: Effects of Fibres Length and Fibres Loading Towards the Composites Flexural and Morphological Properties," *Journal of Mechanical Engineering* 19, no. 2 (2022): 147–167, https://doi.org/10.24191/jmeche.v19i2.19769.

23. S. Picken, A. Korobko, E. Mendes, et al., "Mechanical and Thermal Properties of Polymer Micro- and Nanocomposites," *Journal of Polymer Engineering* 31, no. 2-3 (2011): 269, https://doi.org/10.1515/polyeng.2011.054.

24. R. Pal, "On the Lewis–Nielsen Model for thermal/Electrical Conductivity of Composites," *Composites Part A: Applied Science and Manufacturing* 39, no. 5 (2008): 718–726, https://doi.org/10.1016/j.compositesa.2008.02.008.

25. S. Nejad, "A Review on Modeling of the Thermal Conductivity of Polymeric Nanocomposites," *e-Polymers* 12, no. 1 (2012): 324–339, https://doi.org/10.1515/epoly.2012.12.1.253.

26. J. Czyzewski, A. Rybak, K. Gaska, R. Sekula, and C. Kapusta, "Modelling of Effective Thermal Conductivity of Composites Filled With Core-Shell Fillers," *Materials* 13, no. 23 (2020): 5480, https://doi.org/10.3390/ma13235480.

27. R. Kochetov, A. Korobko, T. Andritsch, H. P. Morshuis, S. J. Picken, and J. J. Smit, "Three-Phase Lewis-Nielsen Model for the Thermal Conductivity of Polymer Nanocomposites," in *2011 Annual Report Conference on Electrical Insulation and Dielectric Phenomena* (IEEE, 2011), https://doi.org/10.1109/CEIDP.2011.6232664.

28. S. Sreenivasan, S. A. Ibraheem, S. Sulaiman, B. T. H. T. Baharudin, M. K. A. Mohd Ariffin, and K. Abdan, "Evaluation of Combined Treatments of Natural Fibers: Kenaf, Abaca and Oil Palm Fibers Using Micromechanical and SEM Methods," *Advanced Materials Research* 912-914 (2014): 1932–1939, https://doi.org/10.4028/www.scientific.net/AMR.912-914.1932.

29. M. H. Hamidon, M. T. Sultan, A. H. Ahmad, and A. U. H. Shah, "Effects of Fibre Treatment on Mechanical Properties of Kenaf Fibre Reinforced composites: A Review," *Journal of Materials Research and Technology* 8, no. 3 (2019): 3327–3337, https://doi.org/10.1016/j.jmrt.2019.04.012.

30. S. A. Ibraheem, S. Sreenivasan, K. Abdan, S. Sulaiman, A. Ali, and D. L. A. A. Majid, "The Effects of Combined Chemical Treatments on the Mechanical Properties of Three Grades of Sisal," *BioResources* 11, no. 4 (2016): 8968–8980, https://doi.org/10.15376/biores.11.4.8968-8980.

31. S. A. Paul, A. Boudenne, L. Ibos, Y. Candau, J. Kuruvilla, and S. Thomas, "Effect of Fiber Loading and Chemical Treatments on Thermophysical Properties of Banana Fiber/Polypropylene Commingled Composite Materials," *Composites Part A: Applied Science and Manufacturing* 39, no. 9 (2008): 1582–1588, https://doi.org/10.1016/j.compositesa.2008.06.004.

32. M. A. Sawpan, K. L. Pickering, and A. Fernyhough, "Effect of Fibre Treatments on Interfacial Shear Strength of Hemp Fibre Reinforced Polylactide and Unsaturated Polyester Composites," *Composites Part A: Applied Science and Manufacturing* 42, no. 9 (2011): 1189–1196, https://doi.org/10.1016/j.compositesa.2011.05.003.

33. M. Nematollahi, M. Karevan, M. Fallah, and M. Farzin, "Experimental and Numerical Study of the Critical Length of Short Kenaf Fiber Reinforced Polypropylene Composites," *Fibers and Polymers* 21, no. 4 (2020): 821–828, https://doi.org/10.1007/s12221-020-9600-x.

34. N. C. Ecke, J. Höller, J. Niedermeyer, P. Klein, and A. K. Schalrb, "An Adaptation of the Lewis-Nielsen Equations for the Thermal Conductivity of Short Fiber Reinforced Hybrid Composites," *Materials Today Communications* 21 (2019): 100632, https://doi.org/10.1016/j.mtcomm.2019.100632.

35. L. E. Nielsen, "Thermal Conductivity of Particulate-Filled Polymers," *Journal of Applied Polymer Science* 17, no. 12 (1973): 3819–3820, https://doi.org/10.1002/app.1973.070171224.

36. S. Wang, and J. Qiu, "Enhancing Thermal Conductivity of Glass Fiber/Polymer Composites Through Carbon Nanotubes Incorporation," *Composites Part B: Engineering* 41, no. 7 (2010): 533–536, https://doi.org/10.1016/j.compositesb.2010.07.002.

37. K. L. Pickering, M. G. A. Efendy, and T. M. Le, "A Review of Recent Developments in Natural Fibre Composites and Their Mechanical Performance," *Composites Part A: Applied Science and Manufacturing* 83 (2016): 98–112, https://doi.org/10.1016/j.compositesa.2015.08.038.

38. Y. Xie, C. A. S. Hill, Z. Xiao, H. Militz, and C. Mai, "Silane Coupling Agents Used for Natural Fiber/Polymer Composites: A Review," *Composites Part A: Applied Science and Manufacturing* 41, no. 7 (2010): 806–819, https://doi.org/10.1016/j.compositesa.2010.03.005.

39. M. M. Kabir, H. Wang, K. T. Lau, and F. Cardona, "Chemical Treatments on Plant-Based Natural Fibre Reinforced Polymer Composites: An Overview," *Composites Part B: Engineering* 43, no. 7 (2012): 2883–2892, https://doi.org/10.1016/j.compositesb.2012.04.053.

40. F. Agrebi, H. Hammami, M. Asim, M. Jawaid, and A. Kallel, "Impact of Silane Treatment on the Dielectric Properties of Pineapple Leaf/Kenaf Fiber Reinforced Phenolic Composites," *Journal of Composite Materials* 54, no. 7 (2020): 937–946, https://doi.org/10.1177/0021998319871351.

41. P. K. Mallick, *Fiber-Reinforced Composites*, 3rd ed. (CRC Press, 2007), https://doi.org/10.1201/9781420005981.

42. P. S. Neto, J. B. de Oliveira, R. S. de O Buzatti, et al., "Properties Evaluation of Polyester Composites With Fillers for Electrical Sector Applications," *Journal of Materials Science: Composites* 6, no. 1 (2025): 9, https://doi.org/10.1186/s42252-025-00068-8.

43. H. A. Saffian, M. A. Talib, S. H. Lee, et al., "Mechanical Strength, Thermal Conductivity and Electrical Breakdown of Kenaf Core Fiber/Lignin/Polypropylene Biocomposite," *Polymers* 12, no. 8 (2020): 1833, https://doi.org/10.3390/polym12081833.

44. N. Nayak, R. H. N. Reddy, G. Kalagi, and V. Bhat, "Electrical Insulating Properties of Natural Fibre Reinforced Polymer Composites; A Review," *International Journal of Engineering Research & Technology* 6, no. 8 (2017): 165–169, https://doi.org/10.17577/IJERTV6IS080083.

45. M. Jawaid, and H. A. Khalil, "Cellulosic/Synthetic Fibre Reinforced Polymer Hybrid Composites: A Review," *Carbohydrate Polymers* 86, no. 1 (2011): 1–18, https://doi.org/10.1016/j.carbpol.2011.04.043.

46. L. Yan, N. Chouw, and K. Jayaraman, "Flax Fibre and its Composites–A Review," *Composites Part B: Engineering* 56 (2014): 296–317, https://doi.org/10.1016/j.compositesb.2013.08.014.

47. H. M. Akil, M. F. Omar, A. A. M. Mazuki, S. Safiee, Z. A. M. Ishak, and A. Abu Bakar, "Kenaf Fiber Reinforced Composites: A Review," *Materials and Design* 32, no. 8-9 (2011): 4107–4121, https://doi.org/10.1016/j.matdes.2011.04.008.

48. S. Vyazovkin, A. K. Burnham, J. M. Criado, L. A. Pérez-Maqueda, C. Popescu, and N. Sbirrazzuoli, "ICTAC Kinetics Committee Recommendations for Performing Kinetic Computations on Thermal Analysis Data," *Thermochimica Acta* 520, no. 1-2 (2011): 1–19, https://doi.org/10.1016/j.tca.2011.03.034.